Climatology of wavenumber-frequency spectra at the 500mb height along 50 °N during the El Niño/ Southern Oscillation extremes

KLAUS FRAEDRICH and KLAUS MÜLLER, Berlin

Summary. Some effects of the El Niño/Southern Oscillation (ENSO) warm and cold extremes on the mid-latitudes are investigated by a standard circulation statistic of the 500mb geopotential along 50 °N. The stationary and transient eddy variance and the related zonal and wavenumber-frequency decomposition are analysed for nine warm and nine cold events. The results reveal an extratropical ENSO response but also the relatively large variability from event to event.

Klimatologie von Wellenzahl-Frequenz-Spektren der 500mb-Höhe entlang 50 °N bei Extremfällen der El Niño/Southern Oscillation

Zusammenfassung. Eine einfache Zirkulations-Statistik wird auf das 500mb-Geopotential entlang 50 °N (Winter) angewandt, um den Einfluß der El Niño/Southern Oscillation (ENSO) auf die mittleren Breiten zu untersuchen. Für jeweils neun warme und kalte ENSO-Fälle werden die Varianz der stationären und transienten Störungen sowie die Wellenzahl-Frequenz-Spektren analysiert. Die Ergebnisse zeigen zwar Auswirkungen von ENSO auf die mittleren Breiten, aber auch erhebliche Fluktuationen von Fall zu Fall.

1. Introduction

The ENSO signature of the mid-latitude wintertime atmosphere has been analysed by numerous general circulation model (GCM) experiments (see, for example, MECHOSO et al. 1987, GEISLER et al. 1985, PALMER and MANSFIELD 1986a and b) and diagnostic data analyses (see, for example, NAMIAS and CAYAN 1984, VAN LOON and MADDEN 1981, VAN LOON and ROGERS 1981, HOREL and WALLACE 1981). However, there is also evidence that extratropical wintertime circulation anomalies are "more sensitive to certain extratropical sea-surface temperature anomalies than to anomalies associated with El Niño" (WALLACE and JIANG 1986) and that considerable variability characterizes the observed mid-latidude responses on various ENSO extremes. HANSEN et al. (1989) provided a detailed spectral analysis of the mid-latitude geopotential height variance signal due to El Niño. Analysing four warm and three cold ENSO events, they found that the standing variance is stronger in the cold-episode winter composite and weaker in the warm-event composite which is in qualitative agreement with the cold-composite wavenumber 3 (showing higher variance density) plus wavenumber 4, contrasting the reduced contributions by wavenumber 4 (and 3) in the warm-event winter composite for periods longer than ten days. It is the purpose of this note to extend this analysis to a larger sample of nine warm and cold ENSO events to supplement our qualitative approach based on Northern Hemisphere large-scale circulation regimes (DZERDZEEVSKY 1962) responding on ENSO warm and cold events (see, for example, FRAEDRICH et al. 1992), and to bridge the gap to the more comprehensive eddy-mean flow diagnostics, which needs to be applied for the analysis of scale interactions.

2. Data and data-analysis

The longitude and time-dependent geopotential height, $Z(x,t)$, is given by four terms: the zonal-time average attributed to the time-mean meridional circulation; the fluctuations in time of the zonal mean (transient cell); the longitudinal fluctuations of the time averages (stationary eddies); and, finally, the combined zonal-time fluctuations (transient eddies):

$$Z(x,t) = [Z]_{x,t} + ([Z]_x)_t + ([Z]_t)_x + (Z)_{x,t} \qquad (2.1)$$

where the time t and zonal x averages and departures are denoted by $[]_t$, $[]_x$ and $()_t$, $()_x$ respectively. Only the last three terms contribute to the total zonal-time variance, $VarZ(x,t)$, because

$$[Z^2]_{x,t} = [Z]^2_{x,t} + VarZ(x,t) \qquad (2.2)$$

$$VarZ(x,t) = [([Z]_x)^2_t]_{x,t} + [([Z]_t)^2_x]_{x,t} + [(Z)^2_{x,t}]_{x,t} \qquad (2.3)$$

The contributions of the individual terms are the variances of the transient cell (time fluctuations of the zonal mean, first term), the stationary eddies (longitudinal fluctuations of time averages, second term), and the transient eddies (zonal time fluctuations, third term). For each seasonal data set (36 grid points and 120 days, commencing November 1) all terms contributing to the total variance are deduced. Furthermore, the transient eddies of the daily zonal 500mb-geopotential heights are transformed into the zonal wavenumber-frequency domain following the method described by HAYASHI (1973) and applied to northern 500mb-geopotential heights by FRAEDRICH and BÖTTGER (1978). The ENSO

response data set consists of the following nine winter seasons (see, for example, RASMUSSEN and CARPENTER 1983, VAN LOON and SHEA 1985), which commence at the first of November and last 120 days: (i) warm events: 1951/52, 1953/54, 1957/58, 1965/66, 1969/70, 1972/73, 1976/77, 1982/83, 1986/87, (ii) cold events: 1949/50, 1954/55, 1964/65, 1966/67, 1970/71, 1973/74, 1975/76, 1978/79, 1988/89.

3. Zonal circulation statistics: time mean and wavenumber-frequency spectra

Zonal-time mean statistics: The zonal-time statistics of the 500mb geopotential along 50 °N is summarized in Table 1.

(i) The mean cold event is associated with an enhanced transient eddy variance (on the expense of the stationary eddies), whereas the average warm episode tends to smaller transient eddy contributions (equilibrating fluctuations of the transient and stationary eddy variances); the propagating variance is an almost constant part of the transient eddies (about 40 per cent), which hardly changes between the average warm- and cold-event season.

(ii) The mean transient and stationary eddy variances show a 95%-significant warm/cold difference (based on the one-sided t-test). Warm/cold differences can be distinguished on a sufficiently high significance level only for the individual contributions (transient and stationary eddy plus transient cell) but not for the total variance of the geopotential height fluctuations.

Further decompositions of the eddy variances (wavenumber-frequency distributions of the transient eddies) provide additional information about the mid-latitude responses on warm and cold ENSO forcing.

Wavenumber-frequency spectra: Applying the zonal Fourier and time spectral analysis to the geopotential height fluctuations of the transient eddies, $(Z)_{x,t}$, leads to a variance density distribution in a zonal wavenumber-frequency domain. This data transformation follows the procedure described by HAYASHI (1973, see also 1982):

$$[(Z)^2_{x,t}]_{x,t} = \Sigma\,\Sigma\,\{E_z(k,+f) + E_z(k,-f)\} \qquad (3.1)$$

for k,f=0...∞, $E_z(k,\pm f)$ is the two-sided variance density spectrum of the geopotential Z in a wavenumber (k) and frequency(f) domain. It is obtained by first expanding $(Z)_{x,t}$ into zonal Fourier harmonics and then computing power-, co- and quadrature spectra of the cosine (C_k) and sine (S_k) components. The propagating variance density spectrum PR(k,f) is defined by the difference of the eastward and westward contribution of E_z and equals the quadrature spectrum Q_f. It gives the lower limit of travelling wave variance, while the eastward and westward spectra give the upper limit: $PR(k,f)=|Q_f(k,f)|$. The propagation direction can be inferred from the sign of Q_f and means which of the eastward and westward moving component is dominant. If both components are coherent, time fluctuations fixed in longitude (standing fluctuations) result from waves of the same wavenumber and frequency-band travelling in opposite directions. The Fourier harmonics are cut off at wavenumber k=12 beyond which the variance appears to

Table 1. Zonal-time variance of the 500mb geopotential along 50 °N during the winter seasons at the end of (and following) the year of an El Niño/Southern Oscillation warm and cold event: Variances of the transient cell (time fluctuations of the zonal means), the stationary eddies (longitudinal fluctuations of time averages), and the transient eddies (zonal-time fluctuations) are defined in equation (2.3). The total variance of zonal-time fluctuations is the sum of these terms. Propagating variance is part of the transient eddy variance, percentage given in brackets. Geopotential units are in gpdam, the units of variance terms are in gpdam².

Tabelle 1. Zonal zeitliche Varianz des 500mb-Geopotentials entlang 50 °N für die Wintersaisons nach warmen oder kalten ENSO Ereignissen. Die Varianzen der transienten Zelle sowie der stationären und transienten Störungen sind in Gleichung (2.3) definiert. Die Gesamtvarianz der zonal-zeitlichen Fluktuationen entspricht der Summe dieser drei Terme. Die Varianz der wandernden Störungen ist Teil der Varianz der transienten Störungen. Ihr prozentualer Anteil ist in Klammern angegeben. Die Einheit des Geopotentials ist gpdam, die der Varianz gpdam².

Winter	Zonal-time mean of geopotential	Variance of transient cell	Variance of stationary eddies	Variance of transient eddies	Propagating variance		Total variance of zonal-time fluctuations
warm event							
51/52	539.3	24.9	120.3	165.4	58.9	(35.6%)	310.6
53/54	538.0	23.2	125.3	174.8	63.1	(36.1%)	323.3
57/58	538.8	25.5	113.2	154.6	52.9	(34.2%)	293.3
65/66	535.1	21.6	121.2	174.7	68.7	(39.3%)	317.5
69/70	536.8	46.1	163.2	179.2	69.7	(38.9%)	388.5
72/73	537.7	26.8	129.4	201.3	63.9	(31.7%)	357.5
76/77	534.1	29.3	195.2	133.9	51.4	(38.4%)	358.4
82/83	538.3	24.1	165.7	151.4	69.5	(45.9%)	341.2
86/87	537.0	32.1	157.6	153.9	60.8	(39.5%)	343.6
mean	537.2 ± 1.7	28.2 ± 7.4	143.4 ± 27.9	165.5 ± 19.7	62.1 ± 6.8	(37.5%)	337.1 ± 29.1
cold event							
49/50	538.6	28.7	84.8	190.0	55.7	(29.3%)	303.5
54/55	539.6	36.4	118.1	177.2	65.6	(37.0%)	331.7
64/65	538.4	27.7	121.5	202.6	103.5	(51.1%)	351.8
66/67	538.1	53.9	152.1	205.3	63.3	(30.8%)	411.3
70/71	538.2	32.2	89.2	214.4	78.4	(36.6%)	335.8
73/74	537.6	32.3	102.7	206.7	76.2	(36.9%)	341.7
75/76	539.1	33.0	127.9	183.9	80.1	(43.6%)	344.8
78/79	537.2	47.7	91.5	158.1	72.7	(46.0%)	297.3
88/89	538.5	14.3	144.7	162.4	59.3	(36.5%)	321.4
mean	538.4 ± 0.7	34.0 ± 11.5	114.7 ± 24.4	189.0 ± 20.1	72.8 ± 14.4	(39.4%)	337.7 ± 33.1

the negligibly small (<5%). The spectra are computed by using a lag-correlation method up to a 20 day lag. Smoothing is accomplished by applying the Tukey window with an equivalent bandwidth of b=0.0665 cpd and approximately 15 degrees of freedom for each of the 41 spectral estimates. Note that we chose this analysis technique to make our results directly comparable with a corresponding diagnosis of a GCM-model response experiment (MECHOSO et al. 1987); a detailed discussion and evaluation of the various methods of zonal wavenumber-frequency decomposition is given by HANSEN et al. (1989).

The transient eddy variance of the geostrophic meridional wind, $[(V_g)^2_{x,t}]_{x,t}$, is spectrally decomposed in the wavenumber-frequency domain to derive the dominant space and time scales of the mid-latitude motion systems (FRAEDRICH and BÖTTGER 1978) and to evaluate their response on ENSO extremes (MECHOSO et al. 1987, HANSEN et al. 1989). This variance is proportional to the kinetic energy of the meridional geostrophic wind component of the transient eddies. The warm- and cold-event composites of the wavenumber-frequency spectra of the meridional geostrophic wind are presented in Fig. 1a and b, where nine winter averages and the related standard deviations are shown:

Cold-event winters reveal a variance density maximum at the zonal wavenumbers 3 and 4 at periods of 15 days and larger. There is no mean secondary peak at smaller wavelengths. Warm-event winters, however, are associated with a well defined peak at wavenumber 4 (and period of 15 days and more); the quasi-standing wavenumber k=3 peak, which partially contributes to the observed transient eddy variance of the cold events, is clearly absent in the warm event response. Furthermore, a secondary peak appears at wavenumber 7 and period 5 days. The latter characterizes synoptic scale eddies which progress eastward with an average phase speed of about 7.5 ms^{-1}; it is observed in GCM experiments (MECHOSO et al. 1987) where it is not averaged out by the natural variability between individual warm events. However, it should be noted that this is not considered to be a unique warm-event feature in the observational analyses. Finally, these results are in qualitative agreement with the meridional Grosswetter residence time distributions obtained by independent methods and data (FRAEDRICH et al. 1992). Furthermore, the standard deviations (Fig. 1c and d) of the nine warm and nine cold-event winter variance densities provide on error measure; they reveal a wavenumber-frequency structure which is similarly distributed in the wavenumber-frequency domain as that of the averages (Fig. 1b and a). That is, large winter to winter fluctuations occur mainly at large wavelengths and periods during cold-event winters, whereas warm episodes show winter to winter variability in a broader wavenumber-frequency domain.

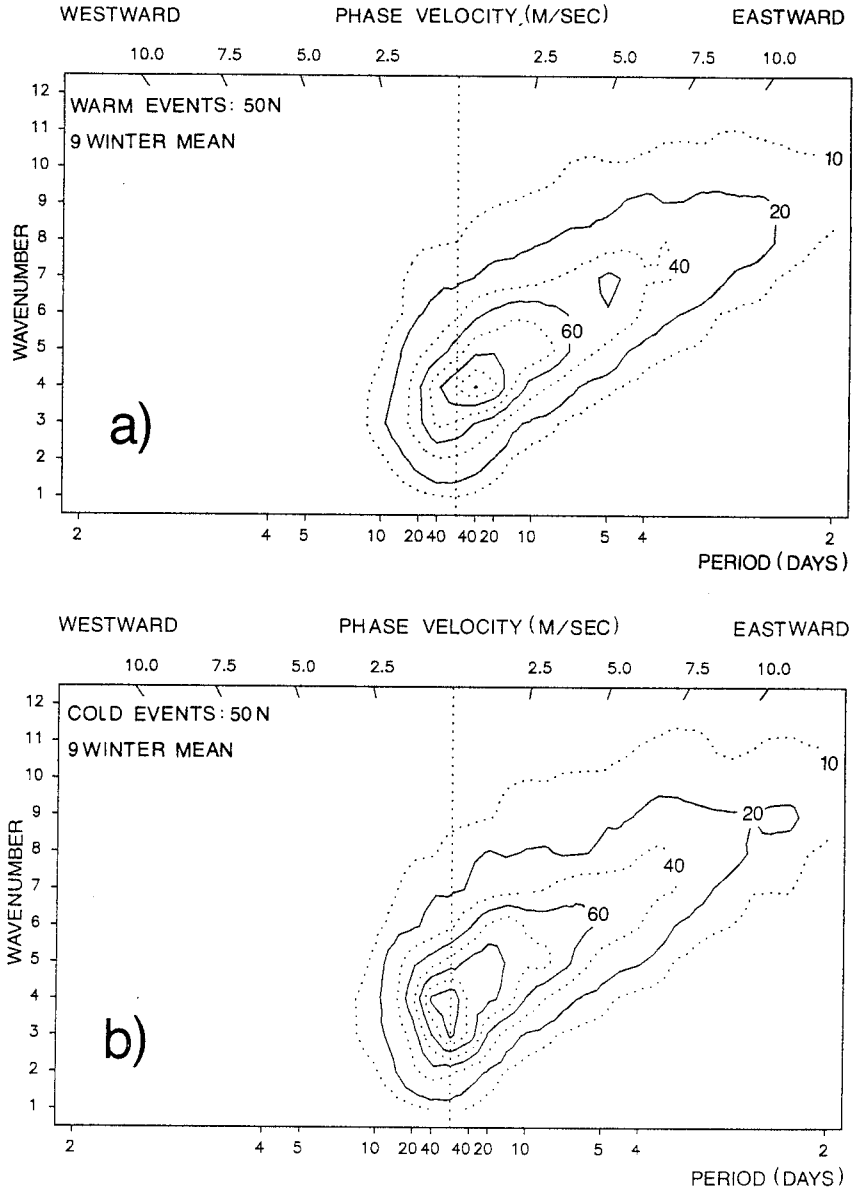

Fig. 1. Transient eddy wavenumber-frequency spectra along 50 °N: Zonal wavenumber-frequency contours of power spectrum density (m^2s^{-2}/df; f: frequency) of the meridional geostrophic wind V_g at 500mb along 50 °N. Nine winter averages are shown for warm (a) and cold (b) extremes of the El Niño/Southern oscillation. The linear frequency axis is labelled in period p of days; the upper abscissa gives the related phase velocity c=L/p in m/s, where L is the wavelength at 50 °N; the c isolines converge at wavenumber k=0 and period p=∞. The standard deviations of the spectral densities are also shown for the nine warm (c) and cold (d) individual winters.

The analysis of the wavenumber-frequency spectra along 40 and 60 °N latitude show a very similar response (not shown) with an enhanced tendency towards retrogression of the longer waves in cold-event winters along the 40 °N latitude circle.

4. Conclusions

The signature of tropical Pacific boundary forcing due to warm and cold ENSO extremes on the mid-latitudes has been investigated by the standard circulation statistics of the winter 500mb-geopotential heights along 50 °N. The tropical Pacific forcing during an ENSO warm/cold-event modifies the transient eddy variance (its zonal and wavenumber decomposition along 50 °N), and the stationary variance. Certain overall features, which are observed in the warm-event composite, can also be found in GCM experiments (MECHOSO et al. 1987, Fig. 16; the variance densities are larger, because the 300 mb-meridional wind is analysed): In comparison with the control run the transient variance density is reduced for wavenumber 3 and 4 and enhanced for wavenumber 6 at a period of about 4 days. Whereas the latter is not considered to be a unique warm-event feature (HANSEN et al. 1989), the differences in the quasi-standing wavenumber k=3 peak are more systematic: They show stronger variance in cold events and are reduced in the warm-episode composite. Finally, it should be mentioned that observational analyses of long distance connections can be evaluated only after the effect and only in a statistical sense due to the system's sensitive dependence on both boundary and initial conditions.

Such zonally averaged diagnostics need to be extended to obtain a more substantial insight into the underlying dynamical processes describing more physical details and feedback mechanisms of the scales involved.

References

Dzerdzeevsky, B., 1962: Fluctuations of climate and the general circulation of the atmosphere in extra-tropical latitudes of the northern Hemisphere and some problems of dynamic climatology. — Tellus **14**, 328—336.

Fraedrich, K., H. Böttger, 1978: A wavenumber-frequency analysis of the 500mb geopotential at 50 °N. — J. Atmos. Sci. **35**, 745—750.

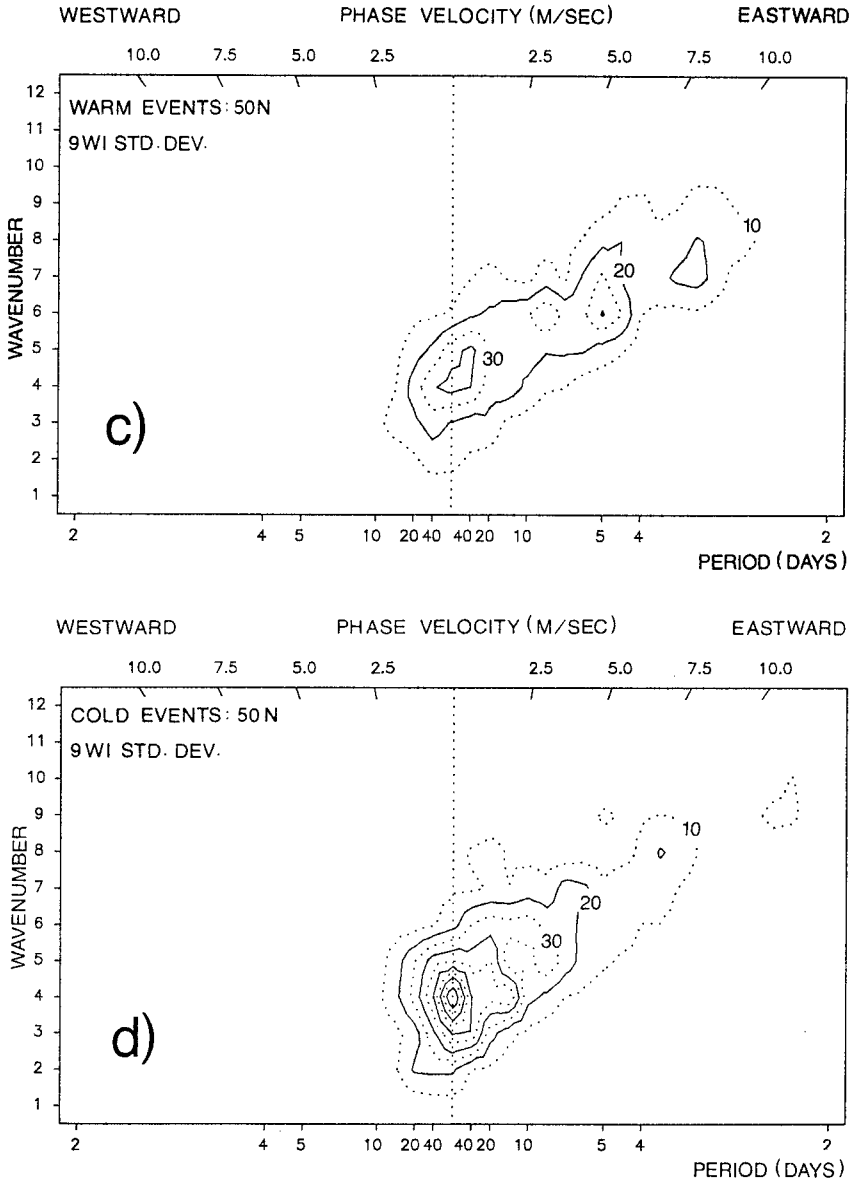

Abb. 1. Wellenzahl-Frequenz-Spektren der transienten Störungen entlang 50 °N: Zonale Wellenzahl-Frequenz-Isolinien der spektralen Dichte ($m^2 s^{-2}$/df, f Frequenz) des meridionalen geostrophischen Windes in 500mb entlang 50 °N. Gezeigt werden die Mittel aus jeweils neun warmen (a) und kalten (b) Winter-Extrema der El Niño/Southern Oscillation. Die untere Abzisse zeigt die Perioden p in Tagen, die obere die Phasengeschwindigkeit c=L/p in m/s, wobei L der Wellenlänge in 50 °N entspricht. Die c-Isolinien konvergieren bei der Wellenzahl k=0 und der Periode p=∞. Die Standardabweichungen der spektralen Dichten werden für die neun warmen (c) und kalten (d) Fälle ebenfalls gezeigt.

Fraedrich, K., K. Müller, R. Kuglin, 1992: Northern hemisphere circulation regimes during the extremes of the El Niño/ Southern Oscillation. — Tellus **44A**, 33—40.

Geisler, J. E., M. L. Blackmon, G. T. Bates, S. Munoz, 1985: Sensitivity of January climate response to the magnitude and position of equatorial Pacific sea surface temperature anomalies. — J. Atmos. Sci. **42**, 1037—1049.

Hansen, A. R., A. Sutera, D. E. Venne, 1989: An examination of midlatitude power spectra: evidence for standing variance and the signature of El Niño. — Tellus **41A**, 371—384.

Hayashi, Y., 1973: A method analysing transient waves by space time cross-spectra. — J. Appl. Meteor. **12**, 404—408.

— 1982: Space-time spectral analysis and its applications to atmospheric waves. — J. Meteor. Soc. Japan **60**, 156—171.

Horel, J. D., J. M. Wallace, 1981: Planetary-scale atmospheric phenomena associated with the Southern Oscillation. — Mon. Wea. Rev. **109**, 813—829.

Mechoso, C. R., A. Kitoh, S. Moorthi, A. Arakawa, 1987: Numerical simulations of the atmospheric resonse to a sea surface temperature anomaly over the equatorial eastern Pacific Ocean. Mon. Wea. Rev. **115**, 2936—2956.

Namias, J., D. R. Cayan, 1984: El Niño: Implications for forecasting. — Oceanus **27**, 41—47.

Palmer, T. N., D. A. Mansfield, 1986a: A study of wintertime circulation anomalies during past El Niño events using a high resolution general Circulation model. I: Influence of model climatology. — Quart. J. R. Met. Soc. **112**, 613—638.

— — 1986b: A study of wintertime circulation anomalies during past El Niño events, using a high resolution general circulation model. II: Variability of the seasonal mean response. — Quart. J. R. Met. Soc. **112**, 947—975.

Rasmusson, E. M., T. H. Carpenter, 1983: The relationship between eastern equatorial Pacific sea surface temperatures and rainfall over India and Sri Lanka. — Mon. Wea. Rev. **111**, 517—528.

van Loon, H., R. A. Madden, 1981: The Southern Oscillation. Part I: Global associations with pressure and temperature in northern winter. — Mon. Wea. Rev. **109**, 1150—1162.

van Loon, H., J. C. Rogers, 1981: The Southern Oscillation. Part II: Associations with changes in the middle troposphere in the northern winter. — Mon. Wea. Rev. **109**, 1163—1168.

van Loon, H., D. J. Shea, 1985: The Southern Oscillation, Part IV: The precursers south of 15 °S to the extremes of the oscillation. — Mon. Wea. Rev. **113**, 2063—2074.

Wallace, J. M., Q. Jiang, 1987: On the observed structure of the interannual variability of the atmosphere/ocean climate system. — In: H. Cattle (Ed.): Atmospheric and Oceanic Variability, 17—43. — Roy. Meteorol. Soc., Bracknell.

KLAUS FRAEDRICH
Meteorologisches Institut
Universität Hamburg
D-2000 Hamburg 13

KLAUS MÜLLER
Institut für Meteorologie
Freie Universität Berlin
D-1000 Berlin 41

Received: 15. 6. 1992, accepted: 22. 6. 1992